Quantitative Short Echo-Time Spectroscopic Imaging at High-Field: Automated Data Reconstruction and LCModel fitting.

R. Otazo[1], J. Alger[2], A. Caprihan[1], T. Li[1], C. Gasparovic[1], S. Posse[1,3]

[1]Mind Imaging Center, University of New Mexico, Albuquerque, NM, United States, [2]Department of Radiology, University of California, Los Angeles, Los Angeles, CA, United States, [3]Psychiatry, University of New Mexico, Albuquerque, NM, United States

Introduction: Short echo-time ^{1}H MR spectroscopic imaging allows the detection of many low-molecular-weight metabolites such as glutamate (Glu) and inositol (Ins), but requires sophisticated fitting approaches for the separation of the metabolite signals due to the spectral overlap and contributions of broad signals with short T_2 that become an underlying baseline [1-2]. The purpose of this study is to show advantages of an automated data processing system to reconstruct short TE Proton-Echo-Planar Spectroscopic Imaging (PEPSI) [3] and conventional SI, and quantification strategies in LCModel [4] to obtain accurate and reproducible fitting.

Methods: Measurements were performed on healthy volunteers using a 4 Tesla Bruker MedSpec scanner, equipped with quadrature head coils. PEPSI data were acquired with TR 2 s and short TE (14 ms), using 32x32 spatial matrix and minimum pixel size of 6 mm. PEPSI encoding consists of alternating odd and even gradient echoes that encode the spatial and spectral information. Complete 8-slice outer volume suppression was applied along the perimeter of the brain. The complete data acquisition includes water suppressed (WS) and non water suppressed (NWS) scans.
Automated data processing was implemented in a graphic data analysis tool written in IDL. The software sorts the odd and even echoes into separate arrays performing time reversal and phase inversion of the odd echo data relative even echo data. This processing produces four distinct t-k_x-k_y arrays (WS-odd, WS-even, NWS-odd, NWS-even). User chosen spatial (Fermi or sine-bell) and time domain (exponential) filters are then applied. Each array is then subjected to 3-dimentional Fast Fourier transform reconstruction to produce four distinct f-x-y arrays. Zero order phases of the water signals are automatically determined in the NWS data and these phase corrections are applied to the corresponding WS data arrays. Spectral frequency assignment in the WS array is made using the NWS data and assuming the largest signal in the NMW data represents water. Fine tuning of the frequency alignment is performed using the NAA peak (2 ppm). Eddy current correction was implemented using the phase information of the NWS data as described in [5]. Water deconvolution is performed by applying a local averaging filter to the time-domain signal and the resulting data set is subtracted from the original data as described in [6]. The software allows the user to view integrated spectral maps and frequency shift maps representing B_0, as well as absorption mode spectra from selected voxels. Time domain data appropriate for LCModel processing are then generated by reverse Fourier transform of each spectrum in the array.
Metabolite quantification is performed by LCModel fitting using empirical constraints in order to obtain consistent results. For frequency referencing in LCModel we used the NAA peak introducing a fixed frequency shift to locate the NAA peak at 2 ppm. No zero-order and first-order phase shifts were allowed and the limit of individual shifts for metabolite spectra was reduced to 0.001 ppm. Cramer-Rao lower bounds were used to assess quality of fit.

Results: High quality spectra were obtained using the IDL software for reconstruction and processing of the PEPSI data (figure 1). Eddy current correction was important to reduce residual line shape distortion and water sidebands in some data. LCModel fitting (figure 2) inside the field of view provided consistent Cramer-Rao lower bounds of: NAA < 3%, Cr < 5%, Cho < 5%, Glu < 9% and Ins < 11%. Similar results were obtained in voxels close to the periphery, despite appreciable susceptibility related line broadening (figure3). Figure 4 shows metabolite concentration maps at 4 T using the concentrations from LCModel.

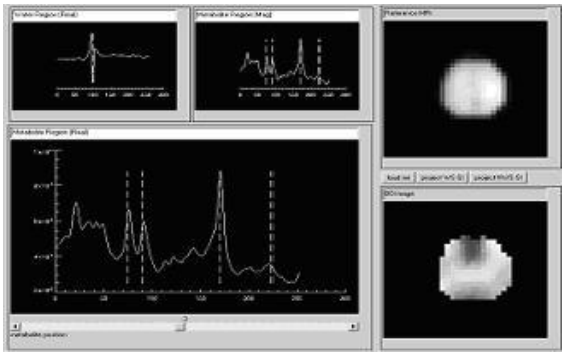

Figure 1: Graphic data analysis tool in IDL, showing the spectra for one voxel, the reference image (NWS data) on the right top and the magnetic field map inside the volume of interest on the bottom right.

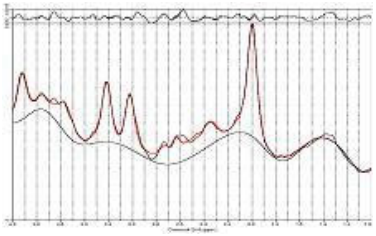

Conc.	%SD	/Cre	Metabolite
0.000	999%	0.000	Ala
0.000	999%	0.000	Asp
1.82E-05	5%	0.480	Cho
3.80E-05	4%	1.000	Cre
6.99E-06	18%	0.184	GABA
0.000	999%	0.000	Gln
1.97E-05	7%	0.520	Glu
0.000	999%	0.000	Gly
8.03E-06	12%	0.211	Ins
4.88E-05	2%	1.285	NAA
0.000	999%	0.000	Tau
2.49E-06	119%	0.066	-CrCH2
3.08E-06	100%	0.081	Gua
1.97E-05	7%	0.520	Glu+Gln

Figure 2: LCModel fitting at 4T (T_E= 14ms). Fit (red line), baseline (black line) and residuals (curve at the top). Concentration table is on the left.

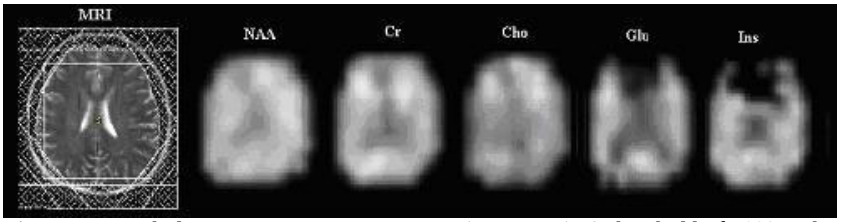

Figure 4: Metabolite concentration maps at 4T (T_E= 14ms). A threshold of 20% to the Cramer-Rao lower bound was used.

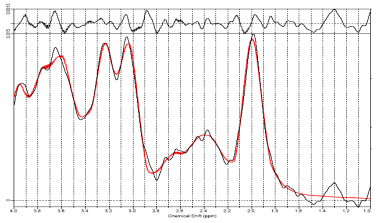

Conc.	%SD	/Cre	Metabolite
0.000	999%	0.000	Ala
6.23E-06	80%	0.083	Asp
2.55E-05	5%	0.338	Cho
7.54E-05	5%	1.000	Cre
3.16E-05	11%	0.419	+GABA
2.15E-05	16%	0.285	Gln
6.78E-06	52%	0.090	Glu
0.000	999%	0.000	Gly
5.49E-05	6%	0.727	Ins
6.37E-05	3%	0.844	NAA
5.29E-05	13%	0.701	+Tau
0.000	999%	0.000	-CrCH2
1.98E-04	7%	2.622	Gua
2.83E-05	14%	0.375	Glu+Gln

Figure 3: LCModel fit of voxel close to the periphery.

Discussion: The reconstruction and processing software and strategies used in LCModel result in consistent and reproducible quantification of metabolites in short TE echo-planar spectroscopic imaging. Whole slice mapping of coupled spin systems is feasible. The accuracy of the fit relies on the quality of the basis set, and we are currently implementing basis sets that include macromolecular signals.

References: [1] J. Pfeuffer *et al*, J. Magn. Reson. **141**, 104-120 (1999). **[2]** L. Hofmann *et al*, Magn. Reson. Med. **48**, 440-453 (2002). **[3]** S. Posse *et al*, Magn. Reson. Med. **33**, 34-40 (1995). **[4]** S. Provencher, Magn. Reson. Imag. **30**, 672-679 (1993). **[5]** U. Klose, Magn. Reson. Imag. **14**, 26-30 (1990). **[6]** D. Marion *et al*, J. Magn. Reson. **84**, 425-430 (1989). *Supported by NIDA 1 R01 DA14178-0 and the MIND Institute*